Effect of *n*- and *p*-type dopants on patterned amorphous regrowth

S. Morarka[a)]
Department of Electrical and Computer Engineering, University of Florida, 216 Larsen Hall, Gainesville, Florida 32611-6200

N. G. Rudawski
Department of Materials Science and Engineering, University of Florida, Gainesville, Florida 32611-6400

M. E. Law
Department of Electrical and Computer Engineering, University of Florida, 216 Larsen Hall, Gainesville, Florida 32611-6200

K. S. Jones
Department of Materials Science and Engineering, University of Florida, Gainesville, Florida 32611-6400

R. G. Elliman
Department of Electronic Materials Engineering, Research School of Physical Sciences and Engineering, Australian National University, Canberra ACT 0200, Australia

(Received 10 June 2009; accepted 27 July 2009; published 3 March 2010)

Solid-phase epitaxial regrowth for patterned amorphous regions has been known to form device degrading mask-edge defects. Prior studies have shown that orientation dependence of regrowth leads to pinching of the slow regrowing corners (111 fronts) that create these defects [K. L. Saenger *et al.*, J. Appl. Phys. **101**, 104908 (2007)]. Also, the effect of *n*-type and *p*-type dopants on regrowth is known only for 001 bulk [B. C. Johnson and J. C. McCallum, Phys. Res. B **76**, 045216 (2007); J. S. Williams and R. G. Elliman, Phys. Rev. Lett. **51**, 1069 (1983)]. This article studies the effect of these dopants (boron and arsenic) on the patterned amorphous regrowth to see if there is any change in the corner regrowth. The experiment was done on very low resistivity wafers ($\sim 0.003\ \Omega$ cm) so that the doping concentration was constant in the whole amorphous region and the doping was high enough to have a significant effect on the regrowth. Recent studies have also shown that local α-c interface curvature is an important factor in modeling patterned amorphous regrowth for intrinsic Si [S. Morarka *et al.*, J. Appl. Phys. **105**, 053701 (2009)]. This experiment shows the dopant-curvature relationship that is important from modeling perspective. © *2010 American Vacuum Society.*
[DOI: 10.1116/1.3207953]

I. INTRODUCTION

Solid-phase epitaxial regrowth (SPER) of Si occurs during the formation of source and drain regions of complementary metal-oxide-semiconductor (CMOS) devices. SPER leads to the formation of ultrashallow junctions with high dopant activation.[1] Since high doses of dopants are introduced in source and drain regions via ion implantation, in some cases, it leads to amorphization of silicon lattice and SPER is unavoidable.

The macroscopic velocity v of an interface between amorphous (α) and crystalline (c) phases (also referred to as the SPER or regrowth front/interface) is known to be a thermally activated process with an activation energy of $\sim$2.7 eV.[2,3] Additionally, SPER is affected by the crystal orientation of the α-Si/c-Si interface,[2] impurities,[4–8] and the applied mechanical stress.[9–21] Since SPER is of the most technological relevance in source and drain regions generated from patterned α-Si regions with variable crystallographic orientation of the regrowth front, it has to be modeled as a multidimensional process. SPER, in the most general sense, is a three-dimensional (3D) process but in case of one of the dimensions of the structure being very long, it can be effectively treated as a two-dimensional (2D) process. In our study, the pattern is made up of long lines with finite spacing which, in terms of CMOS devices, is effectively equivalent to assuming that the "width" (this corresponds to the dimension into the page in all of the figures) of the transistor is very long, which is a good assumption for many devices. For purposes of simplicity, we have not investigated the 3D case, although it may be relevant in certain situations. Source/drain regrowth involves the presence of dopants that affect the regrowth rate.[3] The experiments done until now to see the effect of dopants on regrowth have been mostly planar (001) samples.[4,5] The dopant related enhancement of regrowth rate has been known to be an electronic process because both *p*-and *n*-type dopants increase the rate when present separately and there is no enhancement when both are present together.[3] The basis for the theory about dopants enhancing the regrowth is that kinklike growth sites of SPER possess electronic energy levels within the band gap. The Fermi level in amorphous silicon is assumed to be pinned at the midband. For aligning of the Fermi levels, the bands on the crystalline side have to bend. The recrystallization velocity is

[a)]Electronic addresses: saurabhm@ufl.edu and saurabhmorarka@gmail.com

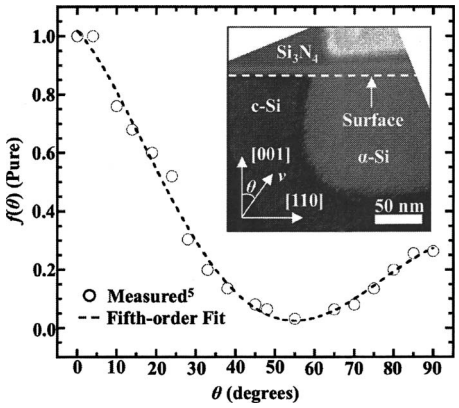

FIG. 1. Normalized SPER velocity, $f(\theta)$, as a function of the substrate orientation angle from [001] toward [110], θ, as measured by Csepregi *et al.* (Ref. 2). The inset shows an XTEM micrograph of a typical 2D structure where the SPER process occurs.

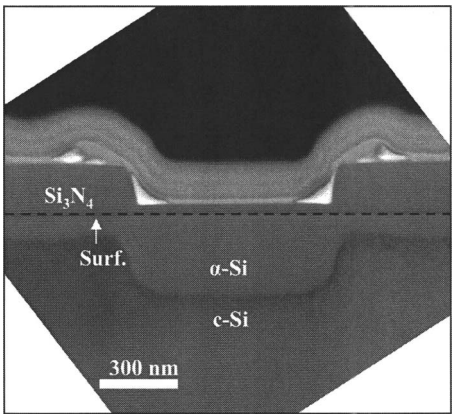

FIG. 2. As-implanted XTEM image for the experiment. Same for semi-insulating, *p*-type and *n*-type samples.

expected to be proportional to the concentration of growth sites. The intrinsic semiconductor's regrowth rate is proportional to the sum of uncharged kink sites C_0 (independent of doping) and charged kink sites (C_i). The doped semiconductor's regrowth rate is proportional to the sum of uncharged kink sites C_0 (independent of doping) and the charged kink sites (C_p). The ratio of charged sites to uncharged sites is Fermi level dependent. Under Maxwell–Boltzmann approximation, the velocity enhancement due to dopant (for *p*-type) is given by[5]

$$F(C_{\mathrm{B}}) = \left[1 + \frac{C_{\mathrm{B}}}{n_i} g \exp\left(-\frac{E_F^i - E_n^p}{kT}\right)\right], \tag{1}$$

where $F(C_{\mathrm{B}})$ is the dopant enhancement factor, E_F^i is the Fermi level in intrinsic material, E_n^p is the energy level at the growth interface of a positively charged defect, C_{B} is the boron concentration at the growth interface, and n_i is the intrinsic carrier concentration at temperature T. The validity of this expression has not been validated for any orientation other than [001]. This is something that is done in this article by using patterned regrowth with constant doping concentration.

Since patterned regrowth is being done, the substrate orientation dependence of SPER is very important to consider. The normalized regrowth velocity, $f(\theta)$, as a function of the substrate orientation angle from [001] toward [110] (θ) was measured by Csepregi *et al.*,[2] as shown in Fig. 1, with the fastest regrowth velocity along [001] [corresponding to $f(\theta)=1.0$]. Thus, v as a function of θ is given by

$$v(\theta) = v_{[001]} f(\theta), \tag{2}$$

where $v_{[001]}$ is the value of v along [001] and $f(\theta)$ is temperature independent and is accurately fit using a least-squares fifth-order polynomial.[22] The [001] regrowth velocity is ~25 times faster than the slowest regrowth direction of [111] and almost ~4 times faster than the [110] direction.

II. EXPERIMENTAL PROCEDURES AND LEVEL SET MODELING

For this work the experimental design was similar to that in Ref. 23. However, a semi-insulating wafer ($\rho \sim 250\ \Omega$ cm) was used as a control for the *p*-type ($\rho \sim 0.003-0.004\ \Omega$ cm) and *n*-type ($\rho \sim 0.003-0.004\ \Omega$ cm) wafers. The *n*-and *p*-type wafers were chosen with very low resistivity to see the maximum effect of dopants on regrowth shapes. Low resistivity wafers were chosen over ion implantation with dopants because ion implantation would have created a Gaussian profile of the dopant in the depth direction. This would lead to a nonuniform regrowth rate enhancement due to the dopants and would make it difficult to draw conclusions about the effect of dopants on the curvature effect.

The 500-μm-thick (001) Si wafers were patterned using masked regions that consisted of lines ~0.5 μm wide. The lines were aligned along the ⟨110⟩ in-plane directions with 150 nm of Si_3N_4 separated by ~0.5 μm wide unmasked area between adjacent lines (Due to some under etch, the unmasked areas had ~20 nm nitride left, as shown in Fig. 2. We will still refer to it as unmasked region for clarity.) All the samples were Si^+ implanted at 20, 60, and 160 keV with doses of 1×10^{15}, 1×10^{15}, and 3×10^{15} cm^{-2} to generate an undulating α-Si layer ~70 nm thick under the masking and ~230 nm thick in the unmasked areas, as shown in Fig. 2. As with the prior experiment,[23] this as-implanted regrowth interface includes both convex and concave curvatures. The regrowth interface is not in contact with any portion of the surface and is therefore not subject to any surface pinning effect which would constrict the regrowth of interface contacting the Si_3N_4.[24]

All the samples were annealed at 500 °C in N_2 ambient. The semi-insulating samples were annealed for 0.5–10.0 h. Annealing times were chosen to see different points during the regrowth process when the regrowth evolution showed important changes. Since, the *n*- and *p*-type dopants are known to increase planar regrowth rates, appropriate annealing times were chosen depending on the doping concentration to catch regrowth at similar points as the semi-insulating

case. Cross-section transmission electron microscopy (XTEM) imaging was used to image the 2D SPER process with XTEM specimens prepared via focused ion beam milling. The 2D SPER process was modeled using level set techniques[25] and implemented in the FLOOPS (Florida object oriented process simulator). Level set simulations have previously been used in etching and deposition simulation and can be readily used to track the velocity of a moving interface with the level set method being very stable regarding the propagation of sharp corners of the interface or merging of two fronts. In simulating SPER, the interface of interest is the α-c interface. More details about level set techniques are presented elsewhere.[22,25] Additionally, the use of FLOOPS provides the advantage of being able to link the regrowth model to the prior diffusion models used in process simulation.

III. RESULTS AND DISCUSSION

Drosd and Washburn[26] showed that the local interfacial curvature κ affects the regrowth rate along [111] and attributed this to the fact that the (111) interface is atomically smooth and should propagate by nucleation and growth of atomic ledges. Hence, if a portion of c-Si is encompassed by α-Si (negative or convex curvature), SPER should be retarded, while if the α-Si is encompassed by c-Si (positive or concave curvature), SPER should be enhanced. Furthermore, it was shown that when the radius of curvature, $r=1/\kappa$, was below ~ 20 μm, a measurable increase in regrowth rate occurred.

Figures 3(a)–3(d) present XTEM images of the 2D SPER process at $T=500$ °C from prior experiment.[23] This experiment was the confirmation for the presence of curvature effect in patterned regrowth. In the presented cases, the growth interface has portions where $r\sim 0.1$ μm. Thus, Eq. (2) was modified to be linearly dependent on the interfacial curvature via

$$v(\theta,\kappa) = v_{[001]} f(\theta)(1 + A\kappa), \tag{3}$$

where A is a constant with units of length. For the presented work, $A=2.0\times 10^{-7}$ cm was used. Equation (2) was used for level set simulation of the 2D SPER process at $T=500$ °C which showed a good matching of simulations with the XTEM images (Fig. 3).

The XTEM images clearly showed the signed curvature effect on regrowth. After regrowing for 2.5 h. [Fig. 3(b)], the convex curvature flattened out, while the concave curvature sharpened. (It should be noted that the concave curvature is the one that increases regrowth velocity due to curvature, however, it still sharpens up. This seems counterintuitive, however, the orientation related effects dominate more than the curvature to create the sharpening corner.) After 5 h, as presented in Fig. 3(c), the pinching of the [111] corner led to the formation of mask-edge defects. Following annealing for 10.0 h, shown in Fig. 3(d), two triangular α-Si regions remained under the mask edge.

Figure 2 shows the as-implanted XTEM image for the experiment that includes both n- and p-type low resistivity

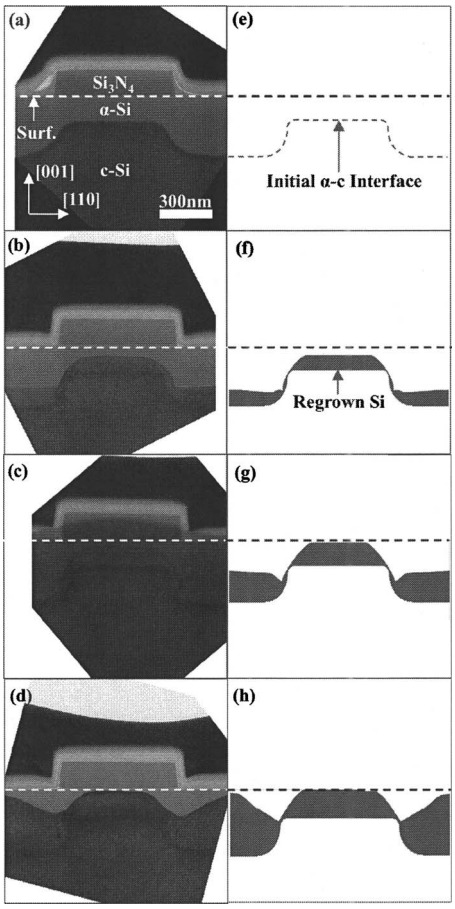

FIG. 3. Observed curvature included simulated 2D SPER process from previous work (Ref. 23) at $T=500$ °C. XTEM images of the structure: (a) as-implanted, (b) after annealing for 2.5 h, (c) after annealing for 5.0 h, and (d) after annealing for 10.0 h. Level set simulations of the structure evolution using both regrowth orientation and interfacial curvature dependence [Eq. (3)]: (e) as-implanted, (f) after annealing for 2.5 h, (g) after annealing for 5.0 h, and (h) after annealing for 10.0 h.

wafers in addition to the semi-insulating (same as-implanted for all three cases). The as-implanted image looks similar to the one from previous experiment.[23] Figures 4(a)–4(c) show the regrowth of semi-insulating sample that is very similar to the previous experiment.[23] The sharpening of the concave corners and flattening of the convex corners is visible. The regrowth however slows down as the interface approaches the surface. Saenger *et al.*[17] explained the slowing down of regrowth below a Si_3N_4 layer to the body effect (arising from the rigidity of Si_3N_4 layer) or a localized increase in α-Si hydrogen concentration. The presence of nitrogen recoils from the ion implantation of Si is possibly responsible for the slowing down as well (since N is known to cause slow regrowth rate[7]). However, the slowing down takes place closer to the surface that is far from the pinching concave corner (the region of interest) so it does not affect the validity of our results.

The results of n-type samples are shown in Figs. 4(d)–4(f). The n-type dopant is arsenic and the doping concentration was found to be $\sim 7\times 10^{19}$ cm^{-3} (from resistivity values). This results in a planar regrowth velocity enhance-

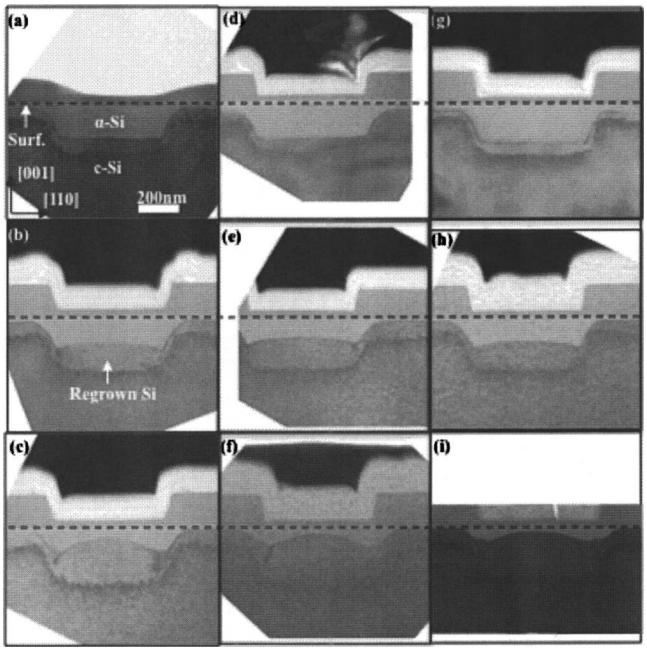

FIG. 4. Observed 2D SPER process at $T=500\,^{\circ}\mathrm{C}$: XTEM images of the structure, semi-insulating [(a)–(c)], (a) after annealing for 2 h, 30 min, (b) after annealing for 5 h, and (c) after annealing for 10 h, *n*-type As samples [(d)–(f)]: (d) after annealing for 1 h, 40 min, (e) after annealing for 3 h, 20 min, and (f) after annealing for 6 h, *p*-type B samples [(g)–(i)]: (g) after annealing for 40 min, (h) after annealing for 1 h, 20 min, and (i) after annealing for 2 h, 40 min.

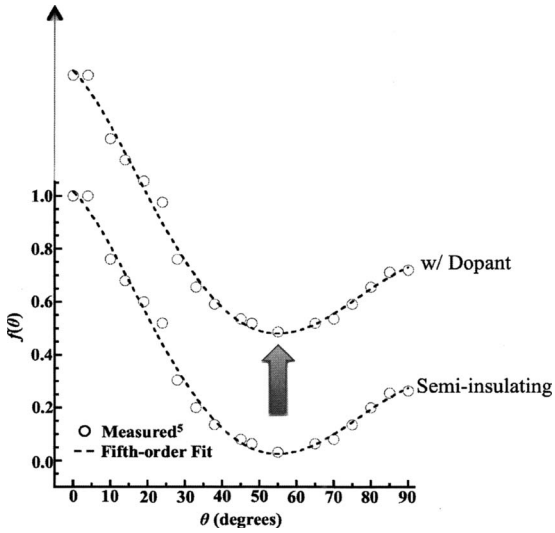

FIG. 5. Data of Csepregi *et al.* (Ref. 2) shifting up due to dopants. Showing an isotropic dopant enhancement effect.

ment of approximately two times. Hence, the regrowth times were chosen to be almost half of the semi-insulating case. The XTEM images show no difference from the semi-insulating case. The same amount of pinching is observed in the concave corners and the defects formed at the same depths.

The *p*-type sample results are shown in Figs. 4(g)–4(i). The *p*-type dopant is boron and the doping concentration was found to be $\sim 4\times 10^{19}\ \mathrm{cm}^{-3}$. This results in a planar regrowth velocity enhancement of approximately four times (can be seen from regrowth times). The XTEM images, like the *n*-type case, show no change in the shape of regrowth. The defects are still formed at the same depth. The last regrowth split at 2 h and 40 min seems a little different from its counterparts because once the mask-edge defects are formed, the regrowth of the defective corner can have some variations. However, it is clear that the regrowth shapes that lead to the pinching of the corner are the same for all cases.

The implication of the regrowth shapes being the same for all three cases is twofold

(1) Dopants increase the planar regrowth rate isotropically (Fig. 5).
(2) The electronic effect that is known to control the enhancement of regrowth rate due to dopants has to be independent of the curvature effect (Fig. 6).

The first conclusion being that the enhancement is isotropic implies that the Csepregi's regrowth data curve shifts upward in the presence of dopants. It also suggests that the defects that are responsible for the rate enhancement are the same for all orientations. This conclusion is understandable because the enhancement is known to be a Fermi level effect.[4,5] Since Fermi level is known to be a function of the material and not the orientation, the results are in conformity with literature.

The second conclusion is that the curvature effect and the dopant "electronic" effect are independent of each other. Figure 6 shows the simulations of varying the curvature parameter (keeping all other parameters constant). As the curvature parameter increases, the pinching of the corner is reduced. No pinching implies no mask-edge defects.

Experimentally, this was found to happen in the presence of an external in-plane unaxial tensile stress[16,27] (higher stresses in corners because of stress-curvature relationship implies stronger effect in the corners). However, no such effect was seen in the presence of dopants only. Hence, Eq. (3) can now be written to include the effect of dopants as

$$v(\theta,\kappa,\mathrm{dopant}) = v_{[001]} f(\theta) F(\mathrm{dopant})(1+A\kappa), \tag{4}$$

where F (dopant) is the Fermi level dependent regrowth rate enhancement given in Eq. (1).

The simulations show that changing the parameter A from 2.0×10^{-7} to 4.0×10^{-7} cm does not make much difference in the regrowth shape. However, increasing A beyond 4.0×10^{-7} cm changes the regrowth shape significantly. When A reaches 8.0×10^{-7} cm (Fig. 6), there is no pinching of the corner. Since the planar regrowth rate enhancement from boron was approximately four times and no change in regrowth shape was seen, curvature effect can be said to be independent of the electronic effect within a reasonable error window. It would be nice to have a much higher dopant effect to make this error smaller. However, with increased doping (for *p*-type dopants such as boron), stress effects from the dopants can start affecting the regrowth as well and that will make it difficult to isolate the different effects.

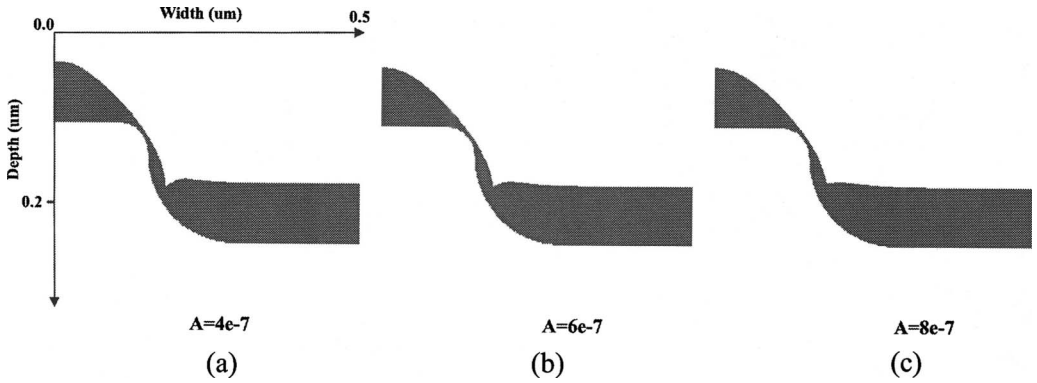

FIG. 6. Level set simulations showing the effect of the curvature parameter A on the shape of regrowth for same time and temperature: (a) $A=4.0\times10^{-7}$ cm (same for $A=2.0\times10^{-7}$ cm), (b) $A=6.0\times10^{-7}$ cm shows less pinching of the [111] corner, and (c) $A=8.0\times10^{-7}$ cm shows no pinching which would mean no mask-edge defect formation.

IV. CONCLUSIONS

The experiment has clearly shown that the SPER rate enhancement due to arsenic and boron is isotropic. The role of curvature effect, in combination with the orientation dependence on the regrowth shapes, was examined and simulations were done using level set methods to see the effect of curvature parameter A on the regrowing shapes. It was also shown that the curvature effect [which is some form of internal stress because of the difference in mechanical properties of amorphous and crystalline Si (Ref. 23)] is independent of the electronic effect that controls the dopant-enhanced regrowth rate.

[1]J. J. Hamilton, E. J. H. Collart, B. Colombeau, C. Jeynes, M. Bersani, D. Giubertoni, J. A. Sharp, N. E. B. Cowern, and K. J. Kirkby, Nucl. Instrum. Methods Phys. Res. B **237**, 107 (2005).
[2]L. Csepregi, E. F. Kennedy, J. W. Mayer, and T. W. Sigmon, J. Appl. Phys. **49**, 3906 (1978).
[3]G. A. Olson and J. A. Roth, Mater. Sci. Rep. **3**, 1 (1988).
[4]B. C. Johnson and J. C. McCallum, Phys. Rev. B **76**, 045216 (2007).
[5]J. S. Williams and R. G. Elliman, Phys. Rev. Lett. **51**, 1069 (1983).
[6]L. Csepregi, E. F. Kennedy, T. J. Gallagher, J. W. Mayer, and T. W. Sigmon, J. Appl. Phys. **48**, 4234 (1977).
[7]E. F. Kennedy, L. Csepregi, J. W. Mayer, and T. W. Sigmon, J. Appl. Phys. **48**, 4241 (1977).
[8]J. C. McCallum, Nucl. Instrum. Methods Phys. Res. B **148**, 350 (1999).
[9]G. Q. Lu, E. Nygren, M. J. Aziz, D. Turnbull, and C. W. White, Appl. Phys. Lett. **54**, 2583 (1989).
[10]E. Nygren, M. J. Aziz, D. Turnbull, J. M. Poate, D. C. Jacobson, and R. Hull, Appl. Phys. Lett. **47**, 232 (1985).
[11]N. G. Rudawski, K. S. Jones, and R. G. Elliman, J. Vac. Sci. Technol. B **26**, 435 (2008).
[12]N. G. Rudawski, K. S. Jones, and R. Gwilliam, Appl. Phys. Lett. **91**, 172103 (2007).
[13]N. G. Rudawski, K. S. Jones, and R. Gwilliam, Appl. Phys. Lett. **92**, 232110 (2008).
[14]N. G. Rudawski, K. S. Jones, and R. Gwilliam, Mater. Sci. Eng. R. **61**, 40 (2008).
[15]N. G. Rudawski, K. S. Jones, and R. Gwilliam, Phys. Rev. Lett. **100**, 165501 (2008).
[16]N. G. Rudawski, K. N. Siebein, and K. S. Jones, Appl. Phys. Lett. **89**, 082107 (2006).
[17]K. L. Saenger, K. E. Fogel, J. A. Ott, J. P. de Souza, and C. E. Murray, Appl. Phys. Lett. **92**, 124103 (2008).
[18]J. F. Sage, W. Barvosa-Carter, and M. J. Aziz, Appl. Phys. Lett. **77**, 516 (2000).
[19]Y. G. Shin, J. Y. Lee, M. H. Park, and H. K. Kang, Jpn. J. Appl. Phys., Part 1 **40**, 6192 (2001).
[20]Y. G. Shin, J. Y. Lee, M. H. Park, and H. K. Kang, J. Cryst. Growth **233**, 673 (2001).
[21]Y. G. Shin, J. Y. Lee, M. H. Park, and H. K. Kang, J. Cryst. Growth **231**, 107 (2001).
[22]S. Morarka, N. G. Rudawski, and M. E. Law, J. Vac. Sci. Technol. B **26**, 357 (2008).
[23]S. Morarka, N. G. Rudawski, M. E. Law, K. S. Jones, and R. G. Elliman, J. Appl. Phys. **105**, 053701 (2009).
[24]N. Burbure, N. G. Rudawski, and K. S. Jones, Electrochem. Solid-State Lett. **10**, H184 (2007).
[25]J. A. Sethian, *Level Set Methods and Fast Marching Methods: Evolving Interfaces in Computational Geometry, Fluid Mechanics, Computer Vision, and Materials Science*, 2nd ed. (Cambridge University Press, Cambridge, 1999).
[26]B. Drosd and J. Washburn, J. Appl. Phys. **51**, 4106 (1980).
[27]C. Ross and K. S. Jones, Mater. Res. Soc. Symp. Proc. **810**, C10.4.1 (2004).